

Revisiting the $b_1\pi$ and $\rho\pi$ decay modes of the 1^{-+} light hybrid state with light-cone QCD sum rules

Zhuo-Ran Huang^{1,2}, Hong-Ying Jin¹, T.G. Steele² and Zhu-Feng Zhang³

¹Zhejiang Institute of Modern Physics, Zhejiang University, Zhejiang Province, 310027, P. R. China

²Department of Physics and Engineering Physics, University of Saskatchewan, Saskatoon, Saskatchewan, S7N 5E2, Canada

³Physics Department, Ningbo University, Zhejiang Province, 315211, P. R. China

We study the $\rho\pi$ and $b_1\pi$ decay modes of the 1^{-+} light hybrid state within the framework of light-cone QCD sum rules. We use both the tensor current $\bar{\psi}\sigma_{\mu\nu}\psi$ and the derivative current $\bar{\psi}\overleftrightarrow{D}_\mu\gamma_5\psi$ as interpolating currents to calculate the partial decay width of the $b_1\pi$ decay mode. Comparing the sum rules obtained by using different currents, we obtain $\Gamma(\pi_1 \rightarrow b_1\pi) = 8-23$, $32-86$ and $52-151$ MeV for $m_{1^{-+}} = 1.6$, 1.8 and 2.0 GeV respectively, which favour the results from the flux tube models and lattice simulations. We also use the tensor current to study the $\rho\pi$ decay mode, and although an extended stability criterion is needed, our results suggest a small partial decay width.

PACS numbers: 12.38.Lg, 12.39.Mk, 14.40.Rt

I. INTRODUCTION

The 1^{-+} light hybrid mesons have attracted particular attention in hadronic physics. The reason is not only such a state can be distinguished from ordinary $q\bar{q}$ mesons for its beyond-quark-model exotic quantum number but also it is expected to be one of the lowest-lying hybrid states. To date, accumulated experimental data have shown the existence of 1^{-+} isovector states, i.e. $\pi_1(1400)$, identified in $\eta\pi$ and $\eta'\pi$ channels and $\pi_1(1600)$ seen to decay into $b_1\pi$, $f_1\pi$ and $\eta'\pi$ ¹ [1]. Moreover, there is another 1^{-+} state, $\pi_1(2015)$, quoted in the extended version of PDG [1], which is only observed by E852 in $f_1\pi$ and $b_1\pi$ final states and needs further confirmation.

Computations on the light hybrid spectrum have been conducted with lattice QCD and different phenomenological models (for a review, see [2]). In the bag model, the predicted mass of the low lying 1^{-+} hybrid nonet is around 1.5 GeV [3, 4]. The earliest quenched lattice calculations predicted the 1^{-+} light hybrid mass lies in the region 1.8–2.1 GeV [5–8], while the more recent dynamical calculations predicted the mass is around 2.2 GeV [9, 10]. Isgur and Paton estimated in the flux tube model the 1^{-+} light hybrid mass to be 1.9 GeV [11, 12] while in the constituent gluon models, the exotic light hybrid mass are found to lie in the region 1.8–2.2 GeV [13–15].

In the framework of QCD Sum Rules [16], the earliest leading-order results obtained by different authors show the 1^{-+} light hybrid mass lies in the range 1.6–2.1 GeV [17–23]. Over the past 15 years, different groups extended and improved the sum rule calculation. The radiative corrections were calculated in [24] and [25] for the perturbative terms and in [26] for the OPE. The short distance tachyonic gluon mass effects were also included in [24], and Narison gave a systematical re-examination of the 1^{-+} mass with inclusion of all the previous calculated effects and estimated the mass to be 1.81 GeV [27]. Furthermore, the authors of this paper further complemented the sum rule analysis of the 1^{-+} mass: instanton effects were studied in Zhang's PhD thesis [28], and a monte-carlo based uncertainty analysis was performed in [29]. Both of these efforts show little change in the mass prediction. Moreover, recently we included the higher power corrections of OPE with consideration of operator renormalization [30]. We considered violation of factorization of higher dimensional condensates and updated the QCD input parameters. We obtained a quite conservative range of the 1^{-+} light hybrid mass, i.e. 1.72–2.60 GeV, which only covers $\pi_1(2015)$ and does not support $\pi_1(1600)$ as a pure hybrid. Given that the analysis in [30] has involved all effects that seem to have considerable influence in the sum rule mass extraction, the mass range can be considered as a general conclusion from QCD sum rules.

From the theoretical mass predictions we can see that $\pi_1(1400)$ is not supported to be a hybrid by various theoretical schemes. Even the mass of $\pi_1(1600)$ is lower than many of the theoretical predictions, although this resonance has long been considered as a good hybrid candidate. Some people have argued that $\pi_1(1600)$ can involve a four-quark state, and a mixing of molecular state and four-quark state has been proposed in [27] based on the discussions in [31] and [32] about 1^{-+} tetraquark and molecular states. The unconfirmed $\pi_1(2015)$ has been suggested in [27] and

¹ The situation is uncertain for the $\rho\pi$ decay mode: VES and Compass have not claimed the existence of the $\rho\pi$ decay while some people have argued that the phase motion results observed by E852 can be resulted from the leakage of $\pi_2(1670)$ [1, 2].

[30] to be a good hybrid candidate. To shed further light on the nature of these states needs both theoretical and experimental study of the 1^{-+} decay modes.

The UKQCD collaboration examined the decay of 1^{-+} hybrid with two dynamical quarks in the lattice simulation, and obtained the partial decay widths $\Gamma(\pi_1 \rightarrow b_1\pi) = 400 \pm 120 \text{ MeV}$ and $\Gamma(\pi_1 \rightarrow f_1\pi) = 90 \pm 60 \text{ MeV}$ [10]. Later in [33], Burns and Close found these results agree quite well with the predictions near threshold in the flux tube model, thus they reduced the partial widths to $\Gamma(\pi_1 \rightarrow b_1\pi) \approx 80 \text{ MeV}$ and $\Gamma(\pi_1 \rightarrow f_1\pi) \approx 25 \text{ MeV}$, whereas the results in IKP Model [34, 35] and PSS Model [36, 37] are $\Gamma(\pi_1 \rightarrow b_1\pi) = 51 \text{ MeV}$, $\Gamma(\pi_1 \rightarrow f_1\pi) = 14 \text{ MeV}$ and $\Gamma(\pi_1 \rightarrow b_1\pi) = 40 - 78 \text{ MeV}$, $\Gamma(\pi_1 \rightarrow f_1\pi) = 10 - 18 \text{ MeV}$ respectively. The decay modes of the 1^{-+} light hybrid state have also been studied within the framework of QCD sum rules. The earliest three-point function sum rule studies can be seen in [38] and [21], while a recent study can be seen in [39] where the pion mass terms in the denominator were ignored and only the $1/q^2$ terms divergent in the limit $q^2 \rightarrow 0$ were kept. The authors in [39] also studied the 1^{-+} decay [40] using the light-cone QCD sum rules (LCSR) [41–44], of which the basic idea is to expand the correlation function near the light cone. However, the predicted partial decay width of $\pi_1 \rightarrow b_1\pi$ is somewhat confusing. The suggestion of very tiny decay width of $b_1\pi$ implies both $\pi_1(1600)$ and $\pi_1(2015)$ may not have much of a hybrid constituent, and also doesn't agree with the predictions from various models mentioned above. Considering the important role of $b_1\pi$ decay mode in identifying the 1^{-+} hybrid state, it's worthwhile to re-examine this decay mode within the same theoretical framework.

In this work, we study the $b_1\pi$ decay mode using the b_1 derivative current $\bar{\psi} \overleftrightarrow{D}_\mu \gamma_5 \psi$ instead of the current $\bar{\psi} \overleftrightarrow{\partial}_\mu \gamma_5 \psi$ adopted in [40]. We also use the tensor current $\bar{\psi} \sigma_{\mu\nu} \psi$, which not only couples to b_1 but also the $1^{--} \rho$ meson, thus an analysis of the $\rho\pi$ decay mode can be provided simultaneously. Usually, the ρ meson is studied using the simpler vector interpolating current $\bar{\psi} \gamma_\mu \psi$, as was done in [16, 45] for the mass and in [46, 47] for the decay constant. In addition, attempts to study the ρ meson using the tensor current have also been made previously in both sum rule [48, 49] and lattice calculations [47]. Studies using the tensor current can provide a useful re-examine of the results obtained by using the vector current. Previous sum rule studies using the vector current $\bar{\psi} \gamma_\mu \psi$ predict large partial decay width of $\rho\pi$ channel [39, 40] while this channel is forbidden in the original flux tube model [35] and the partial decay width is still small in its modified versions [36, 37, 50], therefore, it is also worth re-examining this channel by using the tensor current.

We arrange the article as follows: In Sec. II we illustrate the formalism of the light-cone QCD sum rules for deriving the coupling constants in the 1^{-+} decay amplitudes. In Sec. III we present our results of the light-cone expansion of the correlation function of both the tensor current $\bar{\psi} \sigma_{\mu\nu} \psi$ and the derivative current $\bar{\psi} \overleftrightarrow{D}_\mu \gamma_5 \psi$. In Sec. IV we illustrate the method of calculating the integrals of the spectral densities, from which the contribution from excited states and continuum can be subtracted. In Sec. V, we present the numerical analysis of $b_1\pi$ and $\rho\pi$ decay modes with both currents. In Sec. VI we present the summary and conclusions.

II. LIGHT-CONE QCD SUM RULES FOR THE 1^{-+} LIGHT HYBRID STATE

We begin with the following correlation function to study the decay modes $\pi_1 \rightarrow b_1\pi$ and $\pi_1 \rightarrow \rho\pi$:

$$\Pi^{T,D}(k, p) = i \int d^4x e^{ik \cdot x} \langle \pi(q) | T \{ J^{T,D}(x) J^{H\dagger}(0) \} | 0 \rangle, \quad (1)$$

where p , k and q are respectively the momentum for π_1 , b_1 or ρ and π , which satisfy the four-momentum conservation $p = k + q$. $J^H = J_\mu^H = \bar{\psi} G_{\mu\nu} \gamma_\nu \psi$ couples to the 1^{-+} light hybrid, $J^T = J_{\mu\nu}^T = \bar{\psi} \sigma_{\mu\nu} \psi$ couples to b_1 and ρ , and $J^D = J_\mu^D = \bar{\psi} \overleftrightarrow{D}_\mu \gamma_5 \psi$ also couples to b_1 .

In the practical calculation, we use $J_\mu^H = \frac{\sqrt{2}}{2}(\bar{u} G_{\mu\nu} \gamma_\nu u - \bar{d} G_{\mu\nu} \gamma_\nu d)$, $J_{\mu\nu}^T = \bar{d} \sigma_{\mu\nu} u$ and $J_\mu^D = \bar{d} \overleftrightarrow{D}_\mu \gamma_5 u$ to study the partial decay widths of decay modes $\pi_1^0 \rightarrow b_1^+ \pi^-$ and $\pi_1^0 \rightarrow \rho^+ \pi^-$, of which the results also hold for $\pi_1^- \rightarrow b_1^0 \pi^+$ and $\pi_1^0 \rightarrow \rho^0 \pi^+$. We define the decay constants through the following formulas:

$$\begin{aligned} \langle 0 | J_\mu^H(0) | \pi_1 \rangle &= f_{\pi_1} m_{\pi_1}^3 \eta_\mu, \quad \langle 0 | J_{\mu\nu}^T(0) | b_1 \rangle = i f_{b_1}^T \epsilon_{\mu\nu\rho\sigma} \epsilon^\rho k^\sigma, \\ \langle 0 | J_{\mu\nu}^T(0) | \rho \rangle &= i f_\rho^T (k_\mu \epsilon_\nu - k_\nu \epsilon_\mu), \quad \langle 0 | J_\mu^D(0) | b_1 \rangle = f_{b_1} \epsilon_\mu, \end{aligned} \quad (2)$$

where ϵ_μ and η_μ are polarization vectors, and the decay amplitudes can be written as:

$$\begin{aligned} \mathcal{M}(\pi_1 \rightarrow \rho\pi) &= i g_\rho \epsilon_{\alpha\beta\rho\sigma} \epsilon^{*\alpha} \eta^\beta k^\rho p^\sigma, \\ \mathcal{M}(\pi_1 \rightarrow b_1\pi) &= i g_{b_1}^1 (\eta \cdot \epsilon^*) + i g_{b_1}^2 (\eta \cdot k) (\epsilon^* \cdot p). \end{aligned} \quad (3)$$

The correlation function can be expanded in the light-cone distribution amplitudes which play the similar role as the condensates of local operators in the SVZ operator product expansion. The light-cone expansions can be compared

to the phenomenological expressions of the correlation function so as to estimate the coupling constants in (3) and then to obtain the partial decay widths. After interpolating the intermediate hadronic states into (1) and using the definitions in (2) and (3), we arrive at the phenomenological sides:

$$\begin{aligned}\Pi_{b_1}^T(k, p) &= i \int d^4x e^{ik \cdot x} \langle \pi^-(q) | T \{ J_{\mu\nu}^T(x) J_{\alpha}^{H^\dagger}(0) \} | 0 \rangle \\ &\rightarrow \frac{f_{\pi_1} f_{b_1}^T}{(p^2 - m_{\pi_1}^2)(k^2 - m_{b_1}^2)} \epsilon_{\mu\nu\rho\sigma} \left[g_{b_1}^1 k^\rho \left(-\frac{p_\alpha p^\sigma}{p^2} + g_\alpha^\sigma \right) + g_{b_1}^2 k^\rho \left(-\frac{k \cdot p}{p^2} p_\alpha p^\sigma + k_\alpha p^\sigma \right) \right] + \dots, \quad (4)\end{aligned}$$

$$\begin{aligned}\Pi_\rho^T(k, p) &= i \int d^4x e^{ik \cdot x} \langle \pi^-(q) | T \{ J_{\mu\nu}^T(x) J_{\alpha}^{H^\dagger}(0) \} | 0 \rangle \\ &\rightarrow g_\rho \frac{f_{\pi_1} f_\rho^T}{(p^2 - m_{\pi_1}^2)(k^2 - m_\rho^2)} (-\epsilon_{\rho\sigma\nu\alpha} k^\rho p^\sigma k_\mu + \epsilon_{\rho\sigma\mu\alpha} k^\rho p^\sigma k_\nu) + \dots, \quad (5)\end{aligned}$$

$$\begin{aligned}\Pi_{b_1}^D(k, p) &= i \int d^4x e^{ik \cdot x} \langle \pi^-(q) | T \{ J_\mu^D(x) J_\nu^{H^\dagger}(0) \} | 0 \rangle \\ &\rightarrow \frac{i f_{\pi_1} f_{b_1}}{(p^2 - m_{\pi_1}^2)(k^2 - m_{b_1}^2)} \left[g_{b_1}^1 \left(\frac{k \cdot p k_\mu p_\nu}{k^2 p^2} - \frac{k_\mu k_\nu}{k^2} - \frac{p_\mu p_\nu}{p^2} + g_{\mu\nu} \right) \right. \\ &\quad \left. + g_{b_1}^2 \left(\frac{(k \cdot p)^2 k_\mu p_\nu}{k^2 p^2} - \frac{k \cdot p}{k^2} k_\mu k_\nu - \frac{k \cdot p}{p^2} p_\mu p_\nu + p_\mu k_\nu \right) \right] + \dots, \quad (6)\end{aligned}$$

where the ellipses denote the contribution from excited states and continuum.

On the QCD side, the correlation function (1) can be expanded near the light-cone $x^2 = 0$ in terms of meson distribution amplitudes of different twists. After picking out characteristic tensor structures we get invariant parts of correlation functions corresponding to different coupling constants in (4)–(6). Sometimes this process involves some technical complications as different tensor structures entangle with each other at first sight. We will discuss these details in the next section.

In order to subtract the contribution from excited states and continuum in the invariants of correlation functions, the double dispersion relation can be used:

$$\Pi(k^2, p^2) = \int_0^\infty ds_1 \int_0^\infty ds_2 \frac{\rho(s_1, s_2)}{(s_1 - k^2 - i\epsilon)(s_2 - p^2 - i\epsilon)} + \text{subtractions}, \quad (7)$$

where the subtractions eliminate the infinities from the dispersion integral. After taking Borel transformation, which is defined as

$$\mathcal{B}_{k^2}^{M^2} [f(k^2)] = \lim_{n \rightarrow \infty} \frac{(-k^2)^{n+1}}{n!} \left(\frac{d}{dk^2} \right)^n f(k^2) |_{k^2 = -nM^2}, \quad (8)$$

the subtraction terms can be removed and then we get

$$\mathcal{B}_{k^2}^{\frac{1}{\sigma_1}} \mathcal{B}_{p^2}^{\frac{1}{\sigma_2}} \Pi(k^2, p^2) = \int_0^\infty ds_1 \int_0^\infty ds_2 e^{-s_1 \sigma_1} e^{-s_2 \sigma_2} \rho(s_1, s_2), \quad (9)$$

from which we can subtract continuum by cutting the integral at continuum thresholds s_{01} and s_{02} . The spectral density $\rho(k^2, p^2)$ can be obtained by taking another double Borel transformations on (9):

$$\rho(s_1, s_2) = \mathcal{B}_{-\sigma_1}^{\frac{1}{s_1}} \mathcal{B}_{-\sigma_2}^{\frac{1}{s_2}} \mathcal{B}_{k^2}^{\frac{1}{\sigma_1}} \mathcal{B}_{p^2}^{\frac{1}{\sigma_2}} \Pi(k^2, p^2). \quad (10)$$

After invoking the double Borel transformations to the phenomenological representations (4), (5) and (6), and compare them with the QCD side (9) using (10), we get the master equations of light-cone QCD sum rules:

$$f_{b_1}^T f_{\pi_1} m_{\pi_1}^3 g_{b_1}^1 e^{-m_{b_1}^2 \sigma_1 - m_{\pi_1}^2 \sigma_2} = \int_0^{s_{01}} ds_1 \int_0^{s_{02}} ds_2 e^{-s_1 \sigma_1} e^{-s_2 \sigma_2} \mathcal{B}_{-\sigma_1}^{\frac{1}{s_1}} \mathcal{B}_{-\sigma_2}^{\frac{1}{s_2}} \mathcal{B}_{k^2}^{\frac{1}{\sigma_1}} \mathcal{B}_{p^2}^{\frac{1}{\sigma_2}} \Pi_{b_1;1}^T(k^2, p^2), \quad (11)$$

$$f_{b_1}^T f_{\pi_1} m_{\pi_1}^3 g_{b_1}^2 e^{-m_{b_1}^2 \sigma_1 - m_{\pi_1}^2 \sigma_2} = \int_0^{s_{01}} ds_1 \int_0^{s_{02}} ds_2 e^{-s_1 \sigma_1} e^{-s_2 \sigma_2} \mathcal{B}_{-\sigma_1}^{\frac{1}{s_1}} \mathcal{B}_{-\sigma_2}^{\frac{1}{s_2}} \mathcal{B}_{k^2}^{\frac{1}{\sigma_1}} \mathcal{B}_{p^2}^{\frac{1}{\sigma_2}} \Pi_{b_1;2}^T(k^2, p^2), \quad (12)$$

$$f_\rho^T f_{\pi_1} m_{\pi_1}^3 g_\rho e^{-m_\rho^2 \sigma_1 - m_{\pi_1}^2 \sigma_2} = \int_0^{s_{01}} ds_1 \int_0^{s_{02}} ds_2 e^{-s_1 \sigma_1} e^{-s_2 \sigma_2} \mathcal{B}_{-\sigma_1}^{\frac{1}{s_1}} \mathcal{B}_{-\sigma_2}^{\frac{1}{s_2}} \mathcal{B}_{k^2}^{\frac{1}{\sigma_1}} \mathcal{B}_{p^2}^{\frac{1}{\sigma_2}} \Pi_\rho^T(k^2, p^2), \quad (13)$$

$$i f_{b_1} f_{\pi_1} m_{\pi_1}^3 g_{b_1}^1 e^{-m_{b_1}^2 \sigma_1 - m_{\pi_1}^2 \sigma_2} = \int_0^{s_{01}} ds_1 \int_0^{s_{02}} ds_2 e^{-s_1 \sigma_1} e^{-s_2 \sigma_2} \mathcal{B}_{-\sigma_1}^{\frac{1}{s_1}} \mathcal{B}_{-\sigma_2}^{\frac{1}{s_2}} \mathcal{B}_{k^2}^{\frac{1}{\sigma_1}} \mathcal{B}_{p^2}^{\frac{1}{\sigma_2}} \Pi_{b_1;1}^D(k^2, p^2), \quad (14)$$

$$i f_{b_1} f_{\pi_1} m_{\pi_1}^3 g_{b_1}^2 e^{-m_{b_1}^2 \sigma_1 - m_{\pi_1}^2 \sigma_2} = \int_0^{s_{01}} ds_1 \int_0^{s_{02}} ds_2 e^{-s_1 \sigma_1} e^{-s_2 \sigma_2} \mathcal{B}_{-\sigma_1}^{\frac{1}{s_1}} \mathcal{B}_{-\sigma_2}^{\frac{1}{s_2}} \mathcal{B}_{k^2}^{\frac{1}{\sigma_1}} \mathcal{B}_{p^2}^{\frac{1}{\sigma_2}} \Pi_{b_1;2}^D(k^2, p^2), \quad (15)$$

where contributions from excited states and continuum have been subtracted from both phenomenological and QCD sides.

III. LIGHT-CONE EXPANSION OF THE CORRELATION FUNCTIONS

We expand the correlation function near the light-cone in distribution amplitudes calculated in [51]. Contributions of different decay modes mix in the final results. Depending on the certain current used in the correlation function, it is sometimes not quite straightforward to pick out the particular tensor structures corresponding to certain decay modes, which in our case holds for the tensor current. Before presenting our results of light-cone expansion, we show how to separate the tensor structures in the light-cone expansion of correlation functions.

For the tensor current correlation function, the tensors that appear in the final results involve Levi-Civita tensors. Generally we can form six tensor structures with a Levi-Civita tensor and two independent momentums with three independent Lorentz indices μ, ν and α (μ, ν are anti-symmetric). They are

$$\begin{aligned} T_1 &= \epsilon_{\mu\nu\rho\alpha} p^\rho, \quad T_2 = \epsilon_{\mu\alpha\rho\sigma} k^\rho p^\sigma p_\nu - \epsilon_{\nu\alpha\rho\sigma} k^\rho p^\sigma p_\mu, \quad T_3 = \epsilon_{\mu\nu\rho\alpha} k^\rho, \\ T_4 &= \epsilon_{\mu\nu\rho\sigma} k^\rho p^\sigma k_\alpha, \quad T_5 = \epsilon_{\mu\nu\rho\sigma} k^\rho p^\sigma p_\alpha, \quad T_6 = \epsilon_{\mu\alpha\rho\sigma} k^\rho p^\sigma k_\nu - \epsilon_{\nu\alpha\rho\sigma} k^\rho p^\sigma k_\mu. \end{aligned} \quad (16)$$

Actually, only four of the above tensors are independent. One can prove the formula below:

$$T_5 - T_2 = p^2 T_3 - p \cdot k T_1. \quad (17)$$

By exchanging p and k , we get

$$T_4 - T_6 = -k^2 T_1 + p \cdot k T_3. \quad (18)$$

By using (17) and (18), T_1 and T_2 that appear in the final results of the light-cone expansion can be expressed in terms of T_3 – T_6 . On the phenomenological side of correlation function of the tensor current, tensor structures corresponding to different decay modes are as below:

$$\begin{aligned} \pi_1 \rightarrow b_1 \pi &: \quad g_{b_1}^1 \epsilon_{\mu\nu\rho\sigma} k^\rho \left(-\frac{p^\sigma p_\alpha}{p^2} + g_\alpha^\sigma \right) && \sim -\frac{1}{p^2} T_5 + T_3 \\ &+ \quad g_{b_1}^2 \epsilon_{\mu\nu\rho\sigma} k^\rho \left(-\frac{k \cdot p}{p^2} p^\sigma p_\alpha + p^\sigma k_\alpha \right) && \sim -\frac{p \cdot k}{p^2} T_5 + T_4 \\ \pi_1 \rightarrow \rho \pi &: \quad g_\rho (\epsilon_{\rho\sigma\mu\alpha} k^\rho p^\sigma k_\nu - \epsilon_{\rho\sigma\nu\alpha} k^\rho p^\sigma k_\mu) && \sim T_6 \\ 0^{++} \rightarrow b_1 \pi &: \quad g_{b_1}' \epsilon_{\mu\nu\rho\sigma} k^\rho p^\sigma p_\alpha && \sim T_5 \end{aligned} \quad (19)$$

From (19) we can see that T_3 , T_4 and T_6 are the characteristic tensors for $b_1 \pi$ and $\rho \pi$ decay modes, of which the corresponding terms on the QCD side can be extracted to compare with the phenomenological side. After doing this, we obtain the QCD side of the tensor current correlation function with light-cone expansion.

The tensor structure for the correlation function of the derivative current are much simpler, we can see from (6) that $g_{\mu\nu}$ and $p_\mu k_\nu$ can be the characteristic tensors (the 0^{++} decay mode has a tensor structure parallel to p_ν due to $\langle 0 | J_\nu^H(0) | 0^{++} \rangle \sim p_\nu$).

Using the method above, we are able to disentangle the tensor structures and get the following results of light-cone expansion:

$$\mathcal{B}_{k^2}^{\frac{1}{s_1}} \mathcal{B}_{p^2}^{\frac{1}{s_2}} \Pi_{b_1;1}^T(k^2, p^2) = -\frac{\sqrt{2}\pi f_\pi m_\pi^2}{108(m_u + m_d)} \langle \alpha_s G^2 \rangle \left\{ \frac{1}{2} [\phi'_\sigma(u_0) - \phi'_\sigma(\bar{u}_0)] + 3[\phi_p(u_0) + \phi_p(\bar{u}_0)] + 3(\phi_p^{[u]} + \phi_p^{[\bar{u}]}) \right\}, \quad (20)$$

$$\begin{aligned} \mathcal{B}_{k^2}^{\frac{1}{\sigma_1}} \mathcal{B}_{p^2}^{\frac{1}{\sigma_2}} \Pi_{b1;2}^T(k^2, p^2) = & -\frac{\sqrt{2}f_\pi m_\pi^2}{(m_u + m_d)} (\mathcal{T}^{[\alpha_1]} + \mathcal{T}^{[\alpha_2]}) \frac{1}{\sigma} \\ & + \frac{\sqrt{2}\pi f_\pi m_\pi^2}{108(m_u + m_d)} \langle \alpha_s G^2 \rangle \left\{ [\phi_\sigma(u_0) + \phi_\sigma(\bar{u}_0)](\sigma_1 - \sigma_2) + 6(\phi_p^{[u]} + \phi_p^{[\bar{u}]})\sigma_2 \right\}, \end{aligned} \quad (21)$$

$$\mathcal{B}_{k^2}^{\frac{1}{\sigma_1}} \mathcal{B}_{p^2}^{\frac{1}{\sigma_2}} \Pi_\rho^T(k^2, p^2) = \frac{\sqrt{2}\pi f_\pi m_\pi^2}{108(m_u + m_d)} \langle \alpha_s G^2 \rangle \left\{ [\phi_\sigma(u_0) + \phi_\sigma(\bar{u}_0)]\sigma - 6(\phi_p^{[u]} + \phi_p^{[\bar{u}]})\sigma_2 \right\}, \quad (22)$$

$$\mathcal{B}_{k^2}^{\frac{1}{\sigma_1}} \mathcal{B}_{p^2}^{\frac{1}{\sigma_2}} \Pi_{b1;1}^D(k^2, p^2) = \frac{i\sqrt{2}\pi f_\pi m_\pi^2}{108(m_u + m_d)} \left\{ \frac{1}{2} [\phi'_\sigma(u_0) - \phi'_\sigma(\bar{u}_0)] - 3 [\phi_p(u_0) + \phi_p(\bar{u}_0)] \right\} \frac{1}{\sigma} \langle \alpha_s G^2 \rangle, \quad (23)$$

$$\begin{aligned} & \mathcal{B}_{k^2}^{\frac{1}{\sigma_1}} \mathcal{B}_{p^2}^{\frac{1}{\sigma_2}} \Pi_{b1;2}^D(k^2, p^2) \\ = & \frac{i\sqrt{2}\pi f_\pi m_\pi^2}{54(m_u + m_d)} \left\{ (1 - 3u_0 - \frac{\bar{u}_0}{u_0}) [\phi_\sigma(u_0) + \phi_\sigma(\bar{u}_0)] + u_0 \bar{u}_0 [\phi'_\sigma(u_0) - \phi'_\sigma(\bar{u}_0)] \right. \\ & \left. + 3u_0(1 - u_0) [\phi_p(u_0) + \phi_p(\bar{u}_0)] \right\} \langle \alpha_s G^2 \rangle \\ & + \frac{i\sqrt{2}f_\pi m_\pi^2}{(m_u + m_d)} \left[u_0 \mathcal{T}(u_0, \bar{u}_0, 0) + u_0 \mathcal{T}(\bar{u}_0, u_0, 0) + u_0 \left(\frac{\partial \mathcal{T}}{\partial \alpha_3} - \frac{\partial \mathcal{T}}{\partial \alpha_2} \right)^{[\alpha_1]} \right. \\ & \left. + u_0 \left(\frac{\partial \mathcal{T}}{\partial \alpha_3} - \frac{\partial \mathcal{T}}{\partial \alpha_1} \right)^{[\alpha_2]} - \mathcal{T}^{[\alpha_1]} - \mathcal{T}^{[\alpha_2]} \right] \frac{1}{\sigma^2}, \end{aligned} \quad (24)$$

where the Borel variable $\sigma = \sigma_1 + \sigma_2$. We have adopted the vacuum saturation approximation and the definitions of the notations can be found in Appendix A. We have used the same definitions of the pion distribution amplitudes of those used in [40], which have been calculated in [51]. We also use the current $J_\mu^D = \bar{d} \overleftrightarrow{D}_\mu \gamma_5 u$ instead of $\bar{d} \overleftrightarrow{\partial}_\mu \gamma_5 u$ used in [40], which lead to discrepancies in the final results of light-cone expansion and contradictory results in the numerical analysis. We have also compared our results from the non-covariant derivative current with those obtained in [40], only finding a misprint: there are extra u_0 factors in the $\mathcal{T}^{[\alpha_1]}$ and $\mathcal{T}^{[\alpha_2]}$ terms of the light-cone sum rules for g_{b1}^2 in [40].

IV. INTEGRALS OF THE SPECTRAL DENSITIES

After substituting the pion distribution amplitudes with the expressions in Appendix A, $\mathcal{B}_{k^2}^{\frac{1}{\sigma_1}} \mathcal{B}_{p^2}^{\frac{1}{\sigma_2}} \Pi^{T,D}(k^2, p^2)$ in (11)–(15) are of three types: $\frac{\sigma_2^m}{(\sigma_1 + \sigma_2)^n}$, $\ln \frac{\sigma_2}{\sigma_1 + \sigma_2}$ and $\sigma_2 \ln \frac{\sigma_2}{\sigma_1 + \sigma_2}$, where $m \geq 0$ and $n > 0$.

For the first type, the general form of the spectral density integral can be calculated in the following procedure:

$$\begin{aligned} & \int_0^{s_{01}} ds_1 \int_0^{s_{02}} ds_2 e^{-s_1 \sigma_1} e^{-s_2 \sigma_2} \mathcal{B}_{-\sigma_1}^{\frac{1}{\sigma_1}} \mathcal{B}_{-\sigma_2}^{\frac{1}{\sigma_2}} \frac{\sigma_2^m}{(\sigma_1 + \sigma_2)^n} \\ = & \int_0^{s_{01}} ds_1 \int_0^{s_{02}} ds_2 e^{-s_1 \sigma_1} e^{-s_2 \sigma_2} \frac{1}{\Gamma(n)} \frac{\partial^m}{\partial s_2^m} [\delta(s_1 - s_2) s_2^{n-1}] \\ = & \int_0^{s_{01}} ds_1 \int_0^{s_{02}} ds_2 e^{-s_1 \sigma_1} e^{-s_2 \sigma_2} \frac{1}{\Gamma(n)} \frac{\partial^m \delta(s_2 - s_1)}{\partial s_2^m} s_1^{n-1}, \end{aligned} \quad (25)$$

where $s_{01} < s_{02}$ is a reasonable assumption according to $m_{b1,\rho} < m_{\pi_1}$. The power of $\frac{\partial}{\partial s_2}$ in the last equation of (25) can be reduced using integration by parts. Doing this one time, we get the surface term as below:

$$\Delta = \frac{(-1)^m}{\Gamma(n)} \int_0^{s_{01}} ds_1 e^{-s_1 \sigma_1} \frac{\partial^{m-1} \delta(s_1)}{\partial s_1^{m-1}} s_1^{n-1}, \quad (26)$$

which is well-defined and vanishing only if $n > m$. To avoid the ambiguity arising from the surface term, we shift the lower limit of the integral (25) by a small constant and get

$$\begin{aligned}
& \int_{0+}^{s_{01}} ds_1 \int_0^{s_{02}} ds_2 e^{-s_1 \sigma_1} e^{-s_2 \sigma_2} \frac{1}{\Gamma(n)} \frac{\partial^m \delta(s_2 - s_1)}{\partial s_2^m} s_1^{n-1} \\
&= \frac{\sigma_2^m}{\Gamma(n)} \int_0^{s_{01}} ds_1 e^{-s_1(\sigma_1 + \sigma_2)} s_1^{n-1} \\
&= \sigma_2^m (\sigma_1 + \sigma_2)^{-n} \left\{ 1 - \frac{\Gamma[n, (\sigma_1 + \sigma_2)s_{01}]}{\Gamma(n)} \right\} \\
&= \sigma_2^m (\sigma_1 + \sigma_2)^{-n} f_{n-1}[(\sigma_1 + \sigma_2)s_{01}],
\end{aligned} \tag{27}$$

where $f_n(x) = 1 - e^{-x} \sum_{i=0}^n \frac{x^i}{i!}$, $\Gamma[x]$ is the Euler Gamma function, and $\Gamma[x, y]$ is the incomplete Gamma function.

For the second type of the spectral density integrals, we have

$$\begin{aligned}
& \int_0^{s_{01}} ds_1 \int_0^{s_{02}} ds_2 e^{-s_1 \sigma_1} e^{-s_2 \sigma_2} \mathcal{B}_{-\sigma_1}^{\frac{1}{s_1}} \mathcal{B}_{-\sigma_2}^{\frac{1}{s_2}} \ln \frac{\sigma_2}{\sigma_1 + \sigma_2} \\
&= \ln \frac{\sigma_2}{\sigma_1 + \sigma_2} - \int_{s_{01}}^{\infty} ds_1 \int_{s_{02}}^{\infty} ds_2 e^{-s_1 \sigma_1} e^{-s_2 \sigma_2} \mathcal{B}_{-\sigma_1}^{\frac{1}{s_1}} \mathcal{B}_{-\sigma_2}^{\frac{1}{s_2}} \ln \frac{\sigma_2}{\sigma_1 + \sigma_2} \\
&= \ln \frac{\sigma_2}{\sigma_1 + \sigma_2} - \int_{s_{01}}^{\infty} ds_1 \int_{s_{02}}^{\infty} ds_2 e^{-s_1 \sigma_1} e^{-s_2 \sigma_2} \frac{1}{s_2} \delta(s_1 - s_2) \\
&= \ln \frac{\sigma_2}{\sigma_1 + \sigma_2} - \Gamma[0, s_{02}(\sigma_1 + \sigma_2)].
\end{aligned} \tag{28}$$

Similarly, we get the third type of the spectral density integrals:

$$\begin{aligned}
& \int_0^{s_{01}} ds_1 \int_0^{s_{02}} ds_2 e^{-s_1 \sigma_1} e^{-s_2 \sigma_2} \mathcal{B}_{-\sigma_1}^{\frac{1}{s_1}} \mathcal{B}_{-\sigma_2}^{\frac{1}{s_2}} \sigma_2 \ln \frac{\sigma_2}{\sigma_1 + \sigma_2} \\
&= \sigma_2 \ln \frac{\sigma_2}{\sigma_1 + \sigma_2} - \int_{s_{01}}^{\infty} ds_1 \int_{s_{02}}^{\infty} ds_2 e^{-s_1 \sigma_1} e^{-s_2 \sigma_2} \mathcal{B}_{-\sigma_1}^{\frac{1}{s_1}} \mathcal{B}_{-\sigma_2}^{\frac{1}{s_2}} \ln \frac{\sigma_2}{\sigma_1 + \sigma_2} \\
&= \sigma_2 \ln \frac{\sigma_2}{\sigma_1 + \sigma_2} - \int_{s_{01}}^{\infty} ds_1 \int_{s_{02}}^{\infty} ds_2 e^{-s_1 \sigma_1} e^{-s_2 \sigma_2} \frac{1}{s_1} \frac{d}{ds_2} \delta(s_1 - s_2) \\
&= \sigma_2 \ln \frac{\sigma_2}{\sigma_1 + \sigma_2} + e^{-s_{02}(\sigma_1 + \sigma_2)} \frac{1}{s_{02}} - \sigma_2 \Gamma[0, s_{02}(\sigma_1 + \sigma_2)].
\end{aligned} \tag{29}$$

Using these integral formula, we can transform the master equations (11)–(15) into forms of

$$g_{b_1}^1 = \Pi_{b_1;1}^T(\sigma, s_{01}, s_{02}) / (f_{b_1}^T f_{\pi_1} m_{\pi_1}^3 e^{-2m_{b_1}^2 m_{\pi_1}^2 / (m_{b_1}^2 + m_{\pi_1}^2) \cdot \sigma}), \tag{30}$$

$$g_{b_1}^2 = \Pi_{b_1;2}^T(\sigma, s_{01}, s_{02}) / (f_{b_1}^T f_{\pi_1} m_{\pi_1}^3 e^{-2m_{b_1}^2 m_{\pi_1}^2 / (m_{b_1}^2 + m_{\pi_1}^2) \cdot \sigma}), \tag{31}$$

$$g_{\rho} = \Pi_{\rho}^T(\sigma, s_{01}, s_{02}) / (f_{\rho}^T f_{\pi_1} m_{\pi_1}^3 e^{-2m_{\rho}^2 m_{\pi_1}^2 / (m_{\rho}^2 + m_{\pi_1}^2) \cdot \sigma}), \tag{32}$$

$$g_{b_1}^1 = \Pi_{b_1;1}^D(\sigma, s_{01}) / (i f_{b_1} f_{\pi_1} m_{\pi_1}^3 e^{-2m_{b_1}^2 m_{\pi_1}^2 / (m_{b_1}^2 + m_{\pi_1}^2) \cdot \sigma}), \tag{33}$$

$$g_{b_1}^2 = \Pi_{b_1;2}^D(\sigma, s_{01}) / (i f_{b_1} f_{\pi_1} m_{\pi_1}^3 e^{-2m_{b_1}^2 m_{\pi_1}^2 / (m_{b_1}^2 + m_{\pi_1}^2) \cdot \sigma}) \tag{34}$$

respectively, where $\sigma = \sigma_1 + \sigma_2$, and we assume $\frac{\sigma_2}{\sigma_1} = \frac{m_{b_1, \rho}^2}{m_{\pi_1}^2}$.

V. RESULTS AND DISCUSSIONS

To obtain predictions for $g_{b_1}^1$, $g_{b_1}^2$ and g_{ρ} from the master equations (30)–(34), we vary the continuum thresholds s_{01} and s_{02} within the physically acceptable ranges to find the stable regions for the couplings, in which the dependence of the couplings on σ is weak, which allows theoretical predictions. Since there is still different possibilities for the mass of 1^{-+} hybrid, we consider three different values of the hybrid mass, i.e., $m_{\pi_1} = 1.6 \text{ GeV}$, 1.8 GeV and 2.0 GeV , and we use the decay constant $f_{\pi_1} = 0.025 \text{ GeV}$ deduced from QCD sum rules [27, 30].

A. Numerical analysis for $g_{b_1}^1$

We first consider the master equation (30). Numerically we use $m_{b_1} = 1.235 \text{ GeV}$ and $f_{b_1}^T(2 \text{ GeV}) = 0.18 \text{ GeV}$ in [52]. There are two continuum thresholds s_{01} and s_{02} in this sum rule, which seems tricky to deal with. However, we find under $s_{02} > s_{01}$ (given $m_{\pi_1} > m_{b_1, \rho}$), $g_{b_1}^1$ depends weakly on s_{02} (see Figure 1), which enter the sum rules with the incomplete Gamma function. Thus for simplicity, we will set $s_{02} = s_{01} + 1.0 \text{ GeV}^2$ in this sum rule. By varying the value of s_{01} , we can observe how the $g_{b_1}^1 - \sigma$ curves change. In principle, we expect g_{b_1} depend weakly on the external parameters (σ, s_{01}) , which has been emphasized in traditional QCD sum rules [54]. In practice, we find g_{b_1} shows stability in σ (by the extreme values in Figure 2), but no stability in s_{01} . In fact, g_{b_1} increases gradually with s_{01} , which means s_{01} cannot be fixed from the stability criterion. Therefore it is appropriate to consider a conservative range of g_{b_1} by varying s_{01} within its physically acceptable range (where σ stability should also be ensured). In Figure 2, we plot the optimal results obtained in the region $s_{01} = 3 \sim 5 \text{ GeV}^2$. By reading the extremum values for $g_{b_1}^1$ from the curves, we can obtain estimated values for $g_{b_1}^1$. For $m_{\pi_1} = 1.6 \text{ GeV}$, we find $g_{b_1}^1 = -0.12 \sim -0.09 \text{ GeV}$. If the mass of 1^{--} hybrid is larger than 1.6 GeV , we will obtain different values of $g_{b_1}^1$. We find $g_{b_1}^1 = -0.20 \sim -0.15 \text{ GeV}$ for $m_{\pi_1} = 1.8 \text{ GeV}$ and $g_{b_1}^1 = -0.22 \sim -0.17 \text{ GeV}$ for $m_{\pi_1} = 2.0 \text{ GeV}$.

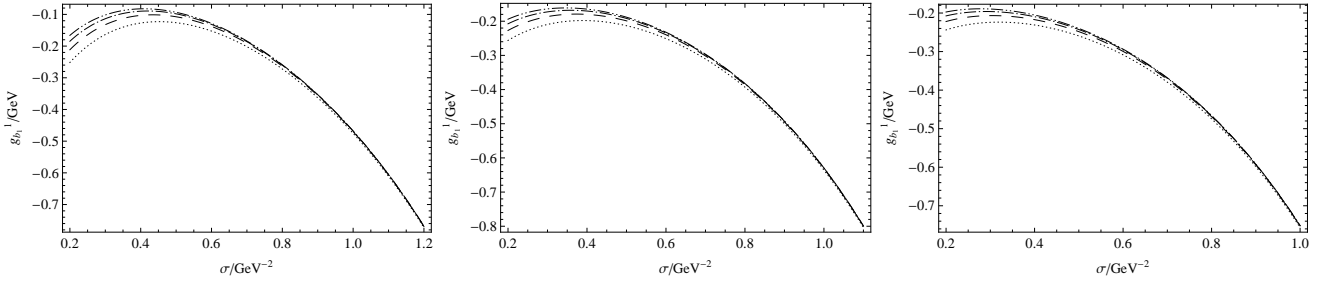


FIG. 1: $g_{b_1}^1 - \sigma$ curves from the master equation (30) for $m_{\pi_1} = 1.6 \text{ GeV}$, $m_{\pi_1} = 1.8 \text{ GeV}$, $m_{\pi_1} = 2.0 \text{ GeV}$. The dotted line, the dashed line, dot-dashed line and the dot-dot-dashed line denote $\{s_{01}, s_{02}\} = \{3 \text{ GeV}^2, 4 \text{ GeV}^2\}$, $\{3 \text{ GeV}^2, 5 \text{ GeV}^2\}$, $\{3 \text{ GeV}^2, 6 \text{ GeV}^2\}$ and $\{3 \text{ GeV}^2, 7 \text{ GeV}^2\}$ respectively.

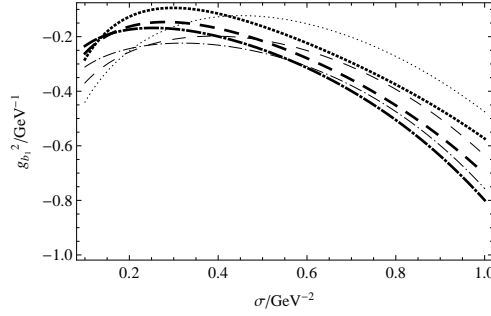


FIG. 2: $g_{b_1}^1 - \sigma$ curves from the master equation (30). The dotted lines, the dashed lines and the dot-dashed lines denote $m_{\pi_1} = 1.6 \text{ GeV}$, 1.8 GeV and 2.0 GeV respectively. All thick lines denote $\{s_{01}, s_{02}\} = \{5 \text{ GeV}^2, 6 \text{ GeV}^2\}$ while the other lines denote $\{s_{01}, s_{02}\} = \{3 \text{ GeV}^2, 4 \text{ GeV}^2\}$.

The sum rule for the derivative current (33) provides a second way to estimate the value of $g_{b_1}^1$, for which we use $f_{b_1}(2 \text{ GeV}) = 0.18 \text{ GeV}$ from [53]. In this sum rule, there is only one continuum threshold s_{01} . However, this sum rule does not reach stability in σ unless we use large values of s_{01} . In Figure 3, we plot curves where stability in σ is initially reached as we increase s_{01} , from which we can read the extreme values of $g_{b_1}^1$, i.e., $g_{b_1}^1 = -0.8 \text{ GeV}$, -0.58 GeV and -0.42 GeV for $m_{\pi_1} = 1.6 \text{ GeV}$, 1.8 GeV and 2.0 GeV respectively. Given that the related s_{01} here lies too far away from the square of the ground state mass, we consider values of $g_{b_1}^1$ from the tensor current LCSR as more reliable predictions.

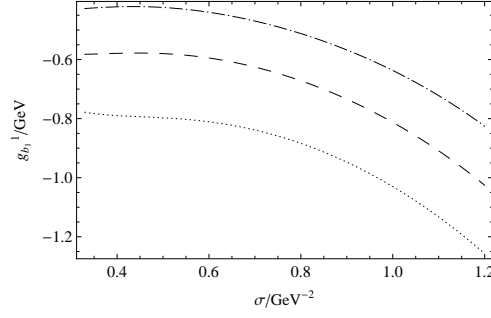


FIG. 3: $g_{b_1}^1 - \sigma$ curve from master equation (33). The dotted line, the dashed line and the dot-dashed line denote $\{s_{01}, m_{\pi_1}\} = \{7 \text{ GeV}^2, 1.6 \text{ GeV}\}$, $\{9 \text{ GeV}^2, 1.8 \text{ GeV}\}$ and $\{11 \text{ GeV}^2, 2.0 \text{ GeV}\}$ respectively.

B. Numerical analysis for $g_{b_1}^2$

To obtain the prediction for $g_{b_1}^2$, we first consider the sum rules for the tensor current. By varying s_{01} and s_{02} , we find $g_{b_1}^2$ is almost insensitive to the value of s_{02} . As can be seen in Figure 4, curves corresponding to the same s_{01} and different s_{02} almost overlap with each other. Thus we can still set $s_{02} = s_{01} + 1.0 \text{ GeV}^2$ in this sum rule.

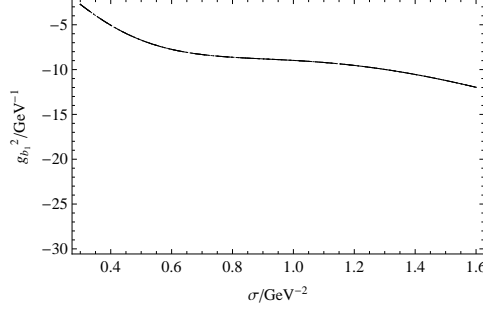


FIG. 4: $g_{b_1}^2 - \sigma$ curves from master equation (31) for $m_{\pi_1} = 1.6 \text{ GeV}$. The dotted line, the dashed line, dot-dashed line and the dot-dot-dashed line denote $\{s_{01}, s_{02}\} = \{5 \text{ GeV}^2, 6 \text{ GeV}^2\}$, $\{5 \text{ GeV}^2, 7 \text{ GeV}^2\}$, $\{5 \text{ GeV}^2, 8 \text{ GeV}^2\}$ and $\{5 \text{ GeV}^2, 9 \text{ GeV}^2\}$ respectively.

In Figure 5, we can observe how the shape of curves change when we increase the value of s_{01} . The curves are monotonous at low s_{01} . If we increase s_{01} , the curves will reach stability in σ . But even as the stability is initially reached, the corresponding s_{01} ($=7, 8, 10 \text{ GeV}^2$ respectively for $m_{\pi_1} = 1.6, 1.8$ and 2.0 GeV) seems too large for the b_1 meson. Therefore we do not intend to extract specific predictions for $g_{b_1}^2$ from LCSR with the tensor current.

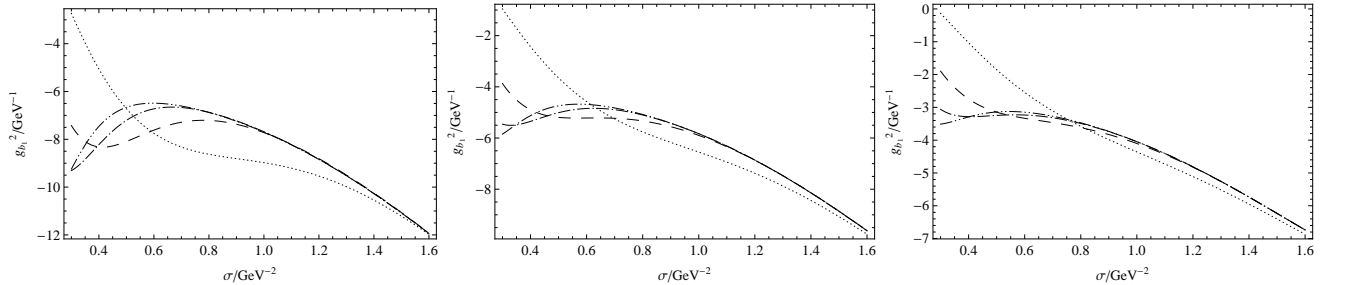


FIG. 5: $g_{b_1}^2 - \sigma$ curves from master equation (31) with $m_{\pi_1} = 1.6, 1.8$ and 2.0 GeV . The dotted line, the dashed line, the dot-dashed line and the dot-dot-dashed line denote $\{s_{01}, s_{02}\} = \{5 \text{ GeV}^2, 6 \text{ GeV}^2\}$, $\{8 \text{ GeV}^2, 9 \text{ GeV}^2\}$, $\{11 \text{ GeV}^2, 12 \text{ GeV}^2\}$ and $\{14 \text{ GeV}^2, 15 \text{ GeV}^2\}$ respectively.

However, the extreme values of the curves will not increase if the value of s_{01} has reached a “huge value”, e.g., 14 GeV^2 for $m_{\pi_1} = 1.6 \text{ GeV}$. which means we can obtain an upper bound of $g_{b_1}^2$. In Figure 5, we obtain $g_{b_1}^2 <$

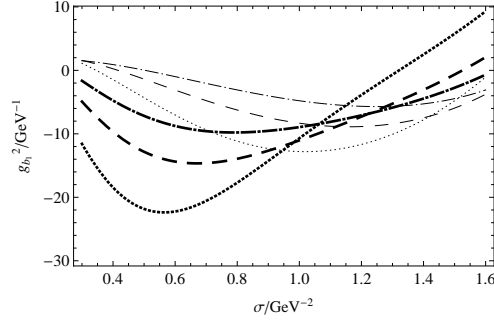


FIG. 6: $g_{b_1}^2 - \sigma$ curves from master equation (34). The dotted lines, the dashed lines and the dot-dashed lines denote $m_{\pi_1} = 1.6$ GeV, 1.8 GeV and 2.0 GeV respectively. All thick lines denote $s_{01} = 5$ GeV² while the other lines denote $s_{01} = 3$ GeV².

-6.5 GeV⁻¹, < -4.5 GeV⁻¹ and < -3 GeV⁻¹ for $m_{\pi_1} = 1.6$ GeV, 1.8 GeV and 2.0 GeV respectively.

The upper bounds above can be compared with the predictions of $g_{b_1}^2$ from using the derivative current, which are obtained from the stability criterion in the region $s_{01} = 3 \sim 5$ GeV². We plot all curves in Figure 6, from which we read $g_{b_1}^2 = -12.8 \sim -22.4$ GeV⁻¹, $-8.9 \sim -14.7$ GeV⁻¹ and $-5.7 \sim -9.8$ GeV⁻¹ for $m_{\pi_1} = 1.6$ GeV, 1.8 GeV and 2.0 GeV respectively.

C. Numerical analysis for g_ρ

By using sum rule for tensor current, we can also try to obtain the prediction for g_ρ . Numerically we adopt $m_\rho = 0.77$ GeV and $f_\rho^T(2 \text{ GeV}) = 0.159$ GeV [47, 48]. Again the coupling is insensitive to the variation of s_{02} when s_{01} is fixed, and we still assume $s_{02} = s_{01} + 1.0$ GeV². As shown in Figure 7, although the sum rules for (32) do not reach exact stability in σ , in the region where the curves are close to stabilizing, there are intersection points for curves with different (s_{01}, s_{02}) . Near these intersection points, g_ρ depends weakly on the variation of (s_{01}, s_{02}) , which fulfills the s_0 stability criterion of which the importance has been emphasized in traditional QCD sum rules [54]. Taking the value of g_ρ at the intersection points, we obtain $g_\rho = -0.06, -0.05$ and -0.06 GeV⁻¹ respectively for 1.6, 1.8 and 2.0 GeV, which suggest g_ρ to be small.

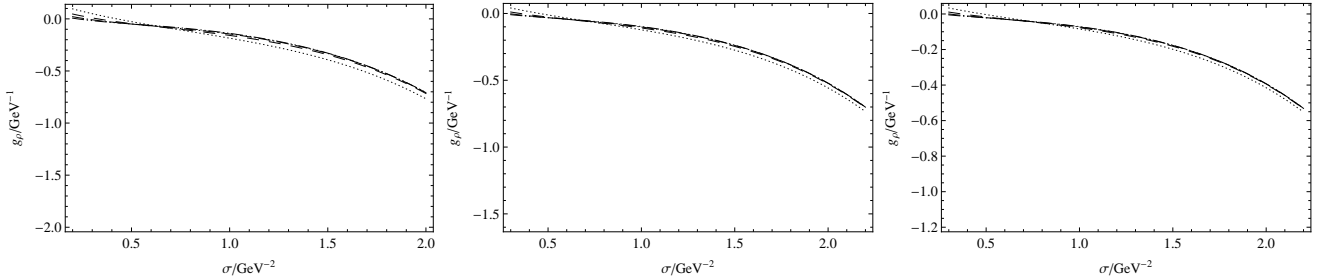


FIG. 7: $g_\rho - \sigma$ curve for $m_{\pi_1} = 1.6$ GeV, 1.8 GeV and 2.0 GeV, from master equation (32). The dotted line, the dashed line, the dot-dashed line and the dot-dot-dashed line denote $\{s_{01}, s_{02}\} = \{2 \text{ GeV}^2, 3 \text{ GeV}^2\}$, $\{3 \text{ GeV}^2, 4 \text{ GeV}^2\}$, $\{4 \text{ GeV}^2, 5 \text{ GeV}^2\}$ and $\{5 \text{ GeV}^2, 6 \text{ GeV}^2\}$ respectively.

D. Decay widths for $\pi_1 \rightarrow b_1 \pi$ and $\pi_1 \rightarrow \rho \pi$

In the previous subsections, we have obtained values and ranges of $g_{b_1}^1$ and $g_{b_1}^2$, from both the tensor current LCSR and derivative current LCSR, and we have also obtained estimates of g_ρ from tensor current LCSR.

Using these values of $g_{b_1}^1$, $g_{b_1}^2$ and g_ρ as our input parameters, we can calculate the decay widths for $\pi_1 \rightarrow b_1 \pi$ and $\pi_1 \rightarrow \rho \pi$ by using

$$\Gamma(\pi_1 \rightarrow b_1^+ \pi^- + b_1^- \pi^+) = \frac{1}{12\pi m_{\pi_1}^2} \cdot \left[(g_{b_1}^1)^2 \left(3 + \frac{k_{b_1}^2}{m_{b_1}^2} \right) k_{b_1} + 2g_{b_1}^1 g_{b_1}^2 \frac{m_{\pi_1}}{m_{b_1}^2} \sqrt{m_{b_1}^2 + k_{b_1}^2} k_{b_1}^3 + (g_{b_1}^2)^2 \frac{m_{\pi_1}^2}{m_{b_1}^2} k_{b_1}^5 \right], \quad (35)$$

and

$$\Gamma(\pi_1 \rightarrow \rho^+ \pi^- + \rho^- \pi^+) = \frac{g_\rho^2}{6\pi} k_\rho^3, \quad (36)$$

respectively, where $k_{b_1/\rho} = \sqrt{[(m_{b_1/\rho} - m_{\pi_1})^2 - m_\pi^2] \cdot [(m_{b_1/\rho} + m_{\pi_1})^2 - m_\pi^2]} / (2m_{\pi_1})$. From these expressions, we obtain possible values and lower bounds of $\Gamma(\pi_1 \rightarrow b_1 \pi)$, which are listed in Table I, from which we can see the predictions from j^D LCSR differs from the very small results obtained in [40]. This discrepancy is mainly due to our addition of the DAs (distribution amplitudes) contribution from the covariant derivative of the current $\bar{\psi} \overleftrightarrow{D}_\mu \gamma_5 \psi$. Since the light-cone expansion is only known to lower twist, inclusion of any contribution is possible to influence the sum rules to a large extent. From the last few subsections, we know that some of the sum rules may suffer from lack of higher twist DAs and are not stable enough within physically acceptable ranges of continuum thresholds, which cause uncertainties in the predictions. From previous analyses, the best sum rules are $g_{b_1}^1$ from j^T LCSR and $g_{b_1}^2$ from j^D LCSR. Therefore we consider the predictions from these sum rules as the most reliable in our calculation. The decay widths are then $\Gamma(\pi_1 \rightarrow b_1 \pi) = 8-23, 32-86$ MeV and $52-151$ for $m_{\pi_1} = 1.6, 1.8$ and 2.0 GeV, which to some extent support the findings from the flux tube model [34–37] and the modified lattice result [33].

	$m_{\pi_1}=1.6$ GeV	$m_{\pi_1}=1.8$ GeV	$m_{\pi_1}=2.0$ GeV
	$\Gamma(\pi_1 \rightarrow b_1 \pi)/\text{MeV}$		
$g_{b_1}^1, g_{b_1}^2$ from j^T LCSR	> 2	> 9	> 16
$g_{b_1}^1, g_{b_1}^2$ from j^D LCSR	20–40	46–103	62–163
$g_{b_1}^1$ from j^T LCSR, $g_{b_1}^2$ from j^D LCSR	8–23	32–86	52–151
$g_{b_1}^1$ from j^D LCSR, $g_{b_1}^2$ from j^T LCSR	> 12	> 18	> 22

TABLE I: Decay widths for $\pi_1 \rightarrow b_1 \pi$.

Using the g_ρ obtained in the last subsection, we obtain $\Gamma(\pi_1 \rightarrow \rho \pi) = 0.021, 0.037$ and 0.040 MeV for $m_{\pi_1} = 1.6, 1.8, 2.0$ GeV, suggesting a small $\rho \pi$ decay width.

VI. SUMMARY AND CONCLUSIONS

We have studied the partial decay widths for decay modes $\pi_1 \rightarrow b_1 \pi$ and $\pi_1 \rightarrow \rho \pi$ using the light-cone QCD sum rules. We use both the tensor current $\bar{\psi} \sigma_{\mu\nu} \psi$ and the derivative current $\bar{\psi} \overleftrightarrow{D}_\mu \gamma_5 \psi$ as interpolating currents in our calculation.

For the $b_1 \pi$ decay mode, we find consistent numerical results (within the errors) of the coupling constants from the sum rules with different interpolating currents. We obtain the partial decay width $\Gamma(\pi_1 \rightarrow b_1 \pi) = 8-23, 32-86$ and $52-151$ MeV for $m_{1-+} = 1.6, 1.8$ and 2.0 GeV respectively from the most reliable sum rules, which provide support for the flux tube model predictions [34–37] and the modified lattice predictions [33]. These results support the hybrid explanations for $\pi_1(1600)$ and $\pi_1(2015)$, both of which have been observed in the $b_1 \pi$ channels.

For the $\rho \pi$ decay mode, we have obtained tiny values of the decay widths, which is quite different from the sum rules obtained by using the vector current $\bar{\psi} \gamma_\mu \psi$. A similar situation also occurs in the sum rules for ρ mass [49]. The authors of [49] attribute this difference to two possible reasons: violation of factorization in estimate of four-quark condensate or weak coupling of the tensor current to the ρ meson. Since the value of the ρ meson decay constant for tensor current obtained from lattice calculation [47] is in a reasonable region, we are inclined towards the first reason. Our results go in line with the predictions obtained from the flux tube model [35–37, 50]. Since the existence of the $\rho \pi$ decay mode is also uncertain for both $\pi_1(1600)$ and $\pi_1(2015)$ in the experiments [1, 2], follow-up studies of this decay mode will be of great help for understanding the nature of these exotic states.

As shown from our calculation, higher twist (in our case, twist-5) DAs contributions may play an important role in stabilizing the sum rules. However, these high twist distribution amplitudes have not been calculated yet. More solid conclusions await the inclusion of contributions from higher twist DAs in the correlation functions.

Acknowledgments

This work is supported by NSFC under grant 11175153, 11205093 and 11347020, and supported by K. C. Wong Magna Fund in Ningbo University. TGS is supported by the Natural Sciences and Engineering Research Council of Canada (NSERC). Z.R. Huang thanks the University of Saskatchewan for its hospitality.

Appendix A: Definitions of Pion Distribution Amplitudes and other notations

The twist-3 light-cone distribution amplitudes of pion $\phi_p(u)$, $\phi_\sigma(u)$ and $\mathcal{T}(\alpha_d, \alpha_u, \alpha_g)$ calculated in [51] are listed below:

$$\langle 0 | \bar{u}(z) i \gamma_5 d(-z) | \pi(P) \rangle = \frac{f_\pi m_\pi^2}{m_u + m_d} \int_0^1 du e^{i(2u-1)pz} \phi_p(u), \quad (37)$$

$$\langle 0 | \bar{u}(z) \sigma_{\alpha\beta} \gamma_5 d(-z) | \pi(P) \rangle = -\frac{i}{3} \frac{f_\pi m_\pi^2}{m_u + m_d} (p_\alpha z_\beta - p_\beta z_\alpha) \int_0^1 du e^{i(2u-1)pz} \phi_\sigma(u), \quad (38)$$

$$\begin{aligned} \langle 0 | \bar{u}(z) \sigma_{\mu\nu} \gamma_5 g_s G_{\alpha\beta}(vz) d(-z) | \pi^-(P) \rangle &= i \frac{f_\pi m_\pi^2}{m_u + m_d} (p_\alpha p_\mu g_{\nu\beta}^\perp - p_\alpha p_\nu g_{\mu\beta}^\perp - p_\beta p_\mu g_{\nu\alpha}^\perp + p_\beta p_\nu g_{\alpha\mu}^\perp) \\ &\quad \int \mathcal{D}\underline{\alpha} e^{-ipz(\alpha_u - \alpha_d + v\alpha_g)} \mathcal{T}(\alpha_d, \alpha_u, \alpha_g), \end{aligned} \quad (39)$$

where the first two DAs are normalized to unity: $\int_0^1 du \phi_{(p,\sigma)}(u) = 1$, and the projector onto the directions orthogonal to p and x is defined as:

$$g_{\mu\nu}^\perp = g_{\mu\nu} - \frac{1}{pz} (p_\mu z_\nu + p_\nu z_\mu), \quad (40)$$

the integration measure is defined as:

$$\int \mathcal{D}\underline{\alpha} = \int_0^1 d\alpha_d d\alpha_u d\alpha_g \delta(1 - \alpha_u - \alpha_d - \alpha_g). \quad (41)$$

The explicit expressions for the DAs calculated in [51] are:

$$\phi_p(u) = 1 + \left(30\eta_3 - \frac{5}{2}\rho_\pi^2\right) C_2^{1/2}(\xi) + \left(-3\eta_3\omega_3 - \frac{27}{20}\rho_\pi^2 - \frac{81}{10}\rho_\pi^2 a_2\right) C_4^{1/2}(\xi), \quad (42)$$

$$\phi_\sigma(u) = 6u(1-u) \left\{ 1 + \left(5\eta_3 - \frac{1}{2}\eta_3\omega_3 - \frac{7}{20}\rho_\pi^2 - \frac{3}{5}\rho_\pi^2 a_2\right) C_2^{3/2}(\xi) \right\}, \quad (43)$$

$$\mathcal{T}(\underline{\alpha}) = 360\eta_3\alpha_u\alpha_d\alpha_g^2 \left\{ 1 + \omega_3 \frac{1}{2}(7\alpha_g - 3) \right\}, \quad (44)$$

where $\xi = 2u - 1$ and $C_n^m(\xi)$ are Gegenbauer polynomials.

Numerically, We use the following values of the light quark masses and the input parameters involved in the light-cone expansion (at $\mu = 1$ GeV) [51, 55]:

$$\begin{aligned} m_\pi^2/(m_u + m_d) &= (1.6 \pm 0.2) \text{ GeV}, \quad m_\pi = 0.134 \text{ GeV}, \quad \rho_\pi^2 \equiv (m_u + m_d)^2/m_\pi^2 \sim O(m_\pi^2), \quad f_\pi = 0.131 \text{ GeV}, \\ a_2 &= 0.44, \quad \eta_3 = 0.015, \quad \omega_3 = -3, \quad \langle \alpha_s G^2 \rangle = 0.07 \text{ GeV}^4. \end{aligned}$$

Some other notations that enter in (20)–(24) are defined as follows:

$$u_0 = \frac{\sigma_2}{\sigma_1 + \sigma_2}, \quad \sigma = \sigma_1 + \sigma_2, \quad \bar{u}_0 = 1 - u_0, \quad \bar{u} = 1 - u, \quad (45)$$

$$\begin{aligned} \phi^{[u]} &= \int_{u_0}^1 \phi(u) \frac{1}{u} du, \quad \phi^{[\bar{u}]} = \int_{u_0}^1 \phi(\bar{u}) \frac{1}{u} du, \\ \mathcal{T}^{[\alpha_1]} &= \int_0^{\bar{u}_0} \mathcal{T}(\alpha_1, u_0, \bar{u}_0 - \alpha_1) d\alpha_1, \\ \mathcal{T}^{[\alpha_2]} &= \int_0^{\bar{u}_0} \mathcal{T}(u_0, \alpha_2, \bar{u}_0 - \alpha_2) d\alpha_2. \end{aligned} \quad (46)$$

-
- [1] K. A. Olive *et al.* [Particle Data Group Collaboration], *Chin. Phys. C* **38**, 090001 (2014).
 - [2] C. A. Meyer and E. S. Swanson, *Prog. Part. Nucl. Phys.* **82**, 21 (2015) [arXiv:1502.07276 [hep-ph]].
 - [3] M. S. Chanowitz and S. R. Sharpe, *Nucl. Phys. B* **222**, 211 (1983) Erratum: [*Nucl. Phys. B* **228**, 588 (1983)].
 - [4] T. Barnes, F. E. Close, F. de Viron and J. Weyers, *Nucl. Phys. B* **224**, 241 (1983).
 - [5] P. Lacock *et al.* [TXL Collaboration], *Nucl. Phys. Proc. Suppl.* **73**, 261 (1999) [hep-lat/9809022].
 - [6] C. McNeile *et al.*, *Nucl. Phys. Proc. Suppl.* **73**, 264 (1999) [hep-lat/9809087].
 - [7] Z. H. Mei and X. Q. Luo, *Int. J. Mod. Phys. A* **18**, 5713 (2003) [hep-lat/0206012].
 - [8] J. N. Hedditch, W. Kamleh, B. G. Lasscock, D. B. Leinweber, A. G. Williams and J. M. Zanotti, *Phys. Rev. D* **72**, 114507 (2005) [hep-lat/0509106].
 - [9] J. J. Dudek, R. G. Edwards, M. J. Peardon, D. G. Richards and C. E. Thomas, *Phys. Rev. D* **82**, 034508 (2010) [arXiv:1004.4930 [hep-ph]].
 - [10] C. McNeile *et al.* [UKQCD Collaboration], *Phys. Rev. D* **73**, 074506 (2006) [hep-lat/0603007].
 - [11] N. Isgur and J. E. Paton, *Phys. Lett. B* **124**, 247 (1983).
 - [12] N. Isgur and J. E. Paton, *Phys. Rev. D* **31**, 2910 (1985).
 - [13] A. Le Yaouanc, L. Oliver, O. Pene, J. C. Raynal and S. Ono, *Z. Phys. C* **28**, 309 (1985).
 - [14] S. Ishida, H. Sawazaki, M. Oda and K. Yamada, *Phys. Rev. D* **47**, 179 (1993).
 - [15] F. Iddir, A. Le Yaouanc, L. Oliver, O. Pene, J. C. Raynal and S. Ono, *Phys. Lett. B* **205**, 564 (1988).
 - [16] M. A. Shifman, A. I. Vainshtein and V. I. Zakharov, *Nucl. Phys. B* **147**, 385 (1979).
 - [17] I. I. Balitsky, D. Diakonov and A. V. Yung, *Phys. Lett. B* **112**, 71 (1982).
 - [18] J. Govaerts, F. de Viron, D. Gusbin and J. Weyers, *Phys. Lett. B* **128**, 262 (1983).
 - [19] I. I. Balitsky, D. Diakonov and A. V. Yung, *Z. Phys. C* **33**, 265 (1986).
 - [20] J. Govaerts, F. de Viron, D. Gusbin and J. Weyers, *Nucl. Phys. B* **248**, 1 (1984).
 - [21] J. I. Latorre, P. Pascual and S. Narison, *Z. Phys. C* **34**, 347 (1987).
 - [22] J. Govaerts, L. J. Reinders, P. Francken, X. Gonze and J. Weyers, *Nucl. Phys. B* **284**, 674 (1987).
 - [23] S. Narison, *Nucl. Phys. A* **675**, 54C (2000) [hep-ph/9909470].
 - [24] K. G. Chetyrkin and S. Narison, *Phys. Lett. B* **485**, 145 (2000) [hep-ph/0003151].
 - [25] H. Y. Jin and J. G. Korner, *Phys. Rev. D* **64**, 074002 (2001) [hep-ph/0003202].
 - [26] H. Y. Jin, J. G. Korner and T. G. Steele, *Phys. Rev. D* **67**, 014025 (2003) [hep-ph/0211304].
 - [27] S. Narison, *Phys. Lett. B* **675**, 319 (2009) [arXiv:0903.2266 [hep-ph]].
 - [28] Zhu-feng Zhang, “QCD Sum Rules, Instanton and New Hadrons (in Chinese)”, Doctoral thesis, Zhejiang University, Hangzhou, China (2008).
 - [29] Z. f. Zhang, H. y. Jin and T. G. Steele, *Chin. Phys. Lett.* **31**, 051201 (2014) [arXiv:1312.5432 [hep-ph]].
 - [30] Z. R. Huang, H. Y. Jin and Z. F. Zhang, *JHEP* **1504**, 004 (2015) [arXiv:1411.2224 [hep-ph]].
 - [31] H. X. Chen, A. Hosaka and S. L. Zhu, *Phys. Rev. D* **78**, 054017 (2008) [arXiv:0806.1998 [hep-ph]].
 - [32] Z. F. Zhang and H. Y. Jin, *Phys. Rev. D* **71**, 011502 (2005) [hep-ph/0412226].
 - [33] T. Burns and F. E. Close, *Phys. Rev. D* **74**, 034003 (2006) [hep-ph/0604161].
 - [34] R. Kokoski and N. Isgur, *Phys. Rev. D* **35**, 907 (1987).
 - [35] N. Isgur, R. Kokoski and J. Paton, *Phys. Rev. Lett.* **54**, 869 (1985) [AIP Conf. Proc. **132**, 242 (1985)].
 - [36] P. R. Page, E. S. Swanson and A. P. Szczepaniak, *Phys. Rev. D* **59**, 034016 (1999) doi:10.1103/PhysRevD.59.034016 [hep-ph/9808346].
 - [37] E. S. Swanson and A. P. Szczepaniak, *Phys. Rev. D* **56**, 5692 (1997) [hep-ph/9704434].
 - [38] F. De Viron and J. Govaerts, *Phys. Rev. Lett.* **53**, 2207 (1984).
 - [39] H. X. Chen, Z. X. Cai, P. Z. Huang and S. L. Zhu, *Phys. Rev. D* **83**, 014006 (2011) [arXiv:1010.3974 [hep-ph]].
 - [40] P. Z. Huang, H. X. Chen and S. L. Zhu, *Phys. Rev. D* **83**, 014021 (2011) [arXiv:1010.2293 [hep-ph]].
 - [41] I. I. Balitsky, V. M. Braun and A. V. Kolesnichenko, *Nucl. Phys. B* **312**, 509 (1989).
 - [42] V. M. Braun and I. E. Filyanov, *Z. Phys. C* **44**, 157 (1989) [*Sov. J. Nucl. Phys.* **50**, 511 (1989)] [*Yad. Fiz.* **50**, 818 (1989)].
 - [43] V. L. Chernyak and I. R. Zhitnitsky, *Nucl. Phys. B* **345**, 137 (1990).
 - [44] V. M. Belyaev, V. M. Braun, A. Khodjamirian and R. Ruckl, *Phys. Rev. D* **51**, 6177 (1995) [hep-ph/9410280].
 - [45] S. Leupold, W. Peters and U. Mosel, *Nucl. Phys. A* **628**, 311 (1998) doi:10.1016/S0375-9474(97)00634-9 [nucl-th/9708016].
 - [46] A. Ali Khan *et al.* [CP-PACS Collaboration], *Phys. Rev. D* **65**, 054505 (2002) Erratum: [*Phys. Rev. D* **67**, 059901 (2003)] doi:10.1103/PhysRevD.65.054505, 10.1103/PhysRevD.67.059901 [hep-lat/0105015].
 - [47] K. Jansen *et al.* [ETM Collaboration], *Phys. Rev. D* **80**, 054510 (2009) [arXiv:0906.4720 [hep-lat]].
 - [48] A. P. Bakulev and S. V. Mikhailov, *Eur. Phys. J. C* **17**, 129 (2000) [hep-ph/9908287].
 - [49] J. Govaerts, L. J. Reinders, F. Deviron and J. Weyers, *Nucl. Phys. B* **283**, 706 (1987).
 - [50] F. E. Close and P. R. Page, *Nucl. Phys. B* **443**, 233 (1995) [hep-ph/9411301].
 - [51] P. Ball, *JHEP* **9809**, 005 (1998) [hep-ph/9802394].
 - [52] K. Jansen *et al.* [ETM Collaboration], *Phys. Lett. B* **690**, 491 (2010) [arXiv:0910.5883 [hep-lat]].
 - [53] L. J. Reinders, H. Rubinstein and S. Yazaki, *Phys. Rept.* **127**, 1 (1985).
 - [54] S. Narison, *Camb. Monogr. Part. Phys. Nucl. Phys. Cosmol.* **17**, 1 (2001) [hep-ph/0205006].
 - [55] S. Narison, *Nucl. Part. Phys. Proc.* **258-259**, 189 (2015) doi:10.1016/j.nuclphysbps.2015.01.041 [arXiv:1409.8148 [hep-ph]].